Available online at www.sciencedirect.com

ScienceDirect

Physics Procedia 56 (2014) 371 – 378

Physics Procedia

8th International Conference on Photonic Technologies LANE 2014

Effects of Defects in Laser Additive Manufactured Ti-6Al-4V on Fatigue Properties

Eric Wycisk[a,*], Andreas Solbach[b], Shafaqat Siddique[c], Dirk Herzog[b], Frank Walther[c], Claus Emmelmann[a,b]

[a] LZN Laser Zentrum Nord GmbH, Am Schleusengraben 14, 21029 Hamburg, Germany
[b] Institut of Laser and System Technologies (iLAS), Hamburg University of Technology (TUHH), Denickestr. 17, 21073 Hamburg, Germany
[c] Department of Materials Test Engineering (WPT), TU Dortmund University, Leonhard-Euler-Str. 5, 44227 Dortmund, Germany

Abstract

Laser Additive Manufacturing (LAM) enables economical production of complex lightweight structures as well as patient individual implants. Due to these possibilities the additive manufacturing technology gains increasing importance in the aircraft and the medical industry. Yet these industries obtain high quality standards and demand predictability of material properties for static and dynamic load cases. However, especially fatigue and crack propagation properties are not sufficiently determined. Therefore this paper presents an analysis and simulation of crack propagation behavior considering Laser Additive Manufacturing specific defects, such as porosity and surface roughness.
For the mechanical characterization of laser additive manufactured titanium alloy Ti-6Al-4V, crack propagation rates are experimentally determined and used for an analytical modeling and simulation of fatigue. Using experimental results from HCF tests and simulated data, the fatigue and crack resistance performance is analyzed considering material specific defects and surface roughness. The accumulated results enable the reliable prediction of the defects influence on fatigue life of laser additive manufactured titanium components.

Peer-review under responsibility of the Bayerisches Laserzentrum GmbH

Keywords: Laser Additive Manufacturing; crack propagation; Kitagawa-Takahashi diagram; El Haddad and Topper; fatigue properties; high cycle fatigue; titanium alloy Ti-6Al-4V

1. Introduction

Layer wise manufacturing technologies such as Laser Additive Manufacturing (LAM) gain increasing importance especially for medical implants and lightweight structures in the aircraft industry. Its unique additive manufacturing process, which permits an economic production of individual and complex parts allowed the laser additive manufacturing technology to be established in industrial applications especially in the medical industry. Its first serial production application is found in the production of dental restorations with a daily production volume of over 10,000 crowns and bridges [Woh13]. Additionally patient individual implants and implants with osseointegrative lattice structures are manufactured with additive manufacturing from titanium alloys [Emm11a]. Already over 20,000 additive manufactured hip implants have been implanted into human bodies [Woh13]. With continuous development of machine technology, adapted design processes and materials for laser additive manufacturing, further

* Corresponding author. Tel.: +49-40-484010-720 ; fax: +49-40-484010-999 .
E-mail address: eric.wycisk@lzn-hamburg.de

Peer-review under responsibility of the Bayerisches Laserzentrum GmbH
doi:10.1016/j.phpro.2014.08.120

applications especially in the aviation industry are at the brim of industrialization [Emm11b]. For these applications in the medical and aviation industry titanium alloys are of highest interest. Especially Ti-6Al-4V due to its good biocompatibility, corrosion resistance and high specific strength is widely used.

However, all existing applications have a predominantly static load case underlying. To widen the possible application spectrum to parts under fatigue loads, considering the high quality and qualification standards of these industries, reliable data on fatigue performance as well as prediction models and simulations have to be established. Recent studies focused on the determination of the fatigue limit of additive manufactured Ti-6Al-4V [Bra10, Wir05, Wyc12, Wyc13]. Due to different manufacturing parameters and post treatment processes in the underlying studies the fatigue limit at $R = 0.1$ varies between 300 MPa and 500 MPa. Further studies on mechanical properties, especially the crack propagation rate were performed by LEUDERS [Leu12] and VAN HOORWEDER [Hoo12]. All previous studies, however, have neglected to investigate in detail the influence of process inherent defects on the fatigue life of additive manufactured Ti-6Al-4V.

In this investigation the effects of defects on the fatigue life was determined and methods for reliable prediction of the fatigue endurance limit analyzed. High cycle fatigue (HCF) tests to determine the fatigue limit and crack propagation tests to investigate the stress intensity threshold ΔK_{th} and crack propagation rates were performed. Defects causing failure in high cycle fatigue tests were identified and measured to assess the influence of the crack size on the endurance limit in a Kitagawa-Takahashi diagram. Additionally LEFM software was used to simulate the influence of surface and volume defects on the endurance limit.

2. Experimental procedures

2.1. Additive manufacturing of test specimen

The manufacturing of all specimens used for this investigation of fatigue limit and crack growth behavior was conducted on a single machine with identical process parameters. Frequent machine maintenance and laser power measurements ensure the process reproducibility across the different manufacturing batches. The specimens were manufactured using a commercially available laser additive manufacturing system with 200 W laser power, a layer thickness of 30 µm and an energy density E of 45.33 J/mm³ under Argon atmosphere. For relaxation of residual stresses, a post-process heat treatment for 3h at 650°C in vacuum with subsequent argon cooling was performed. The specimens were built in upright standing position (90°) with manufacturing layers being perpendicularly orientated to the latter loading direction. Additionally HCF specimens were built with a tilted orientation of 45° to the manufacturing plane.

To investigate the HCF properties of laser additive manufactured Ti-6Al-4V, hour-glass shaped specimens derived from ASTM E 466 [AST07] (Fig. 1) were produced as blanks as well as net-shaped specimens ("as-built" condition). The blanks were machined and polished according to specification, the net-shaped specimens were kept in untreated surface condition with an average surface roughness of R_a = 12 µm. For the determination of the fatigue crack growth rates as well as the threshold value of stress intensity range, compact-tension specimens (CT-specimen) according to ASTM E 647 [AST00] were manufactured. Additive manufactured blanks were machined to final geometry according to the ASTM specifications with an initial crack length of 10 mm (Fig. 1).

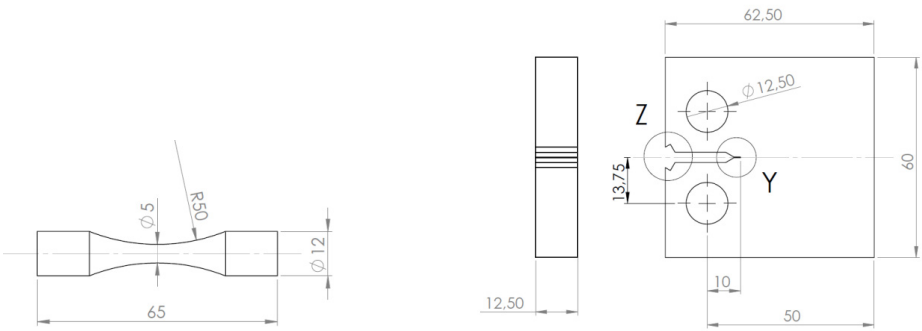

Fig. 1. Hour-glass shaped specimen for HCF tests (left) and CT-specimen for crack propagation tests (right).

2.2. High cycle fatigue tests

High cycle fatigue tests were performed on a servo hydraulic test rig from MTS equipped with a 100 kN load cell and hydraulic clamping jaws. The tests were undertaken in alignment with DIN 50100 [DIN78] at a load ratio of R = 0.1 and a frequency of 50 Hz. Polished and "as-built" specimens in untreated surface conditions were tested to identify the influence of residual porosity and bonding defects as well as surface roughness on the fatigue life of laser additive manufactured Ti-6Al-4V.

2.3. Crack growth rate measurements

To create the Kitagawa-Takahashi diagram (see section 3.4) and simulate the fatigue life with the analytical LEFM software AFGROW (see section 4) it was necessary to determine the crack propagation behavior and the threshold of the stress intensity factor ΔK_{th}. To determine these values, the fatigue crack growth rate has been measured using compact-tension specimen machined as described in section 2.1. The crack propagation tests were conducted on an INSTRON 8801 fatigue testing system equipped with a 100 kN load cell and a 5 mm COD gage with 2 mm travel was employed for monitoring the crack growth behavior. After precracking at constant ΔK to an initial crack length of 13 mm the near threshold region was tested with decreasing ΔK at a rate of – 0.2 mm^{-1} at $R = 0.1$. The Paris regime and higher ΔK values were tested with constant $R = 0.1$ and force of F_{max} = 2300 N. The investigations were performed in strong agreement to ASTM E 647.

3. Experimental results

3.1. High cycle fatigue tests

The HCF test results plotted in a Woehler diagram are shown in Fig. 2. Hollow items symbolize specimen failure, filled items specimen "run out" at 10^7 cycles. An analysis of covariance between different building directions, upright (90°) and tilted (45°), shows no significant effect of the layer orientation on the fatigue performance. Laser additive manufactured Ti-6Al-4V shows an endurance limit of 210 MPa for "as-built" and 500 MPa for polished specimens. "As-built" specimens exhibit a significantly lower endurance limit due to enhanced surface crack initiation on multiple sites (Fig. 3). The additive manufactured material in polished conditions shows high scatter in the region near to the endurance limit. The fracture surface analysis reveals different defect kinds and locations to be responsible for the scatter (compare section 3.2). Further detailed results on HCF tests at $R = 0.1$ of laser additive manufactured Ti-6Al-4V can be found in BRANDL, LEUDERS and WYCISK [Bra10, Leu12, Wyc12, Wy13]

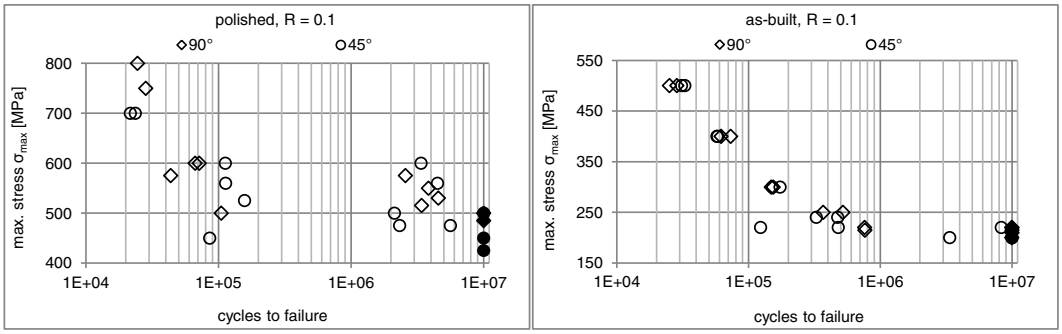

Fig. 2. Woehler diagram for polished (left) and "as-built" specimen (right).

3.2. Fracture surface analysis

The fracture surface analysis with SEM reveals two different crack initiation sites. Internal volume failure, from bonding defects due to insufficient fusion of layers during the manufacturing process, as well as surface failure at the edge of the specimen. Examples of both crack initiation sites are given in Fig. 3.

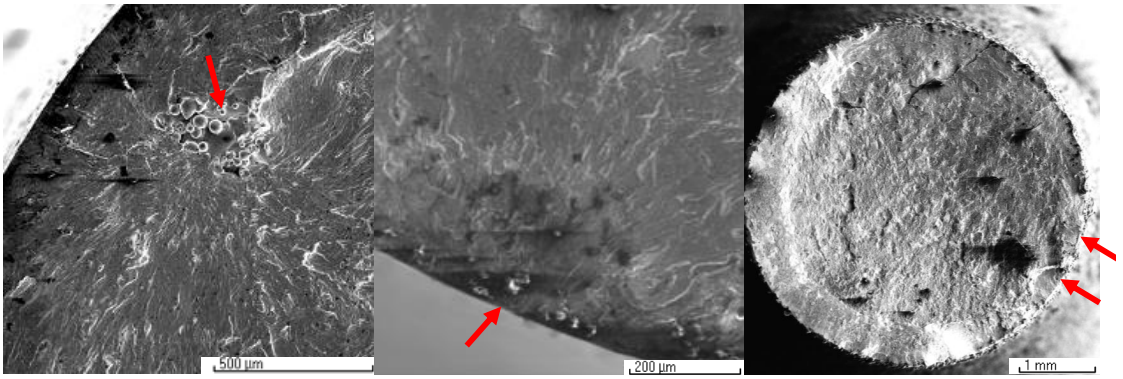

Fig. 3. Fracture surface SEM pictures of polished specimen with crack initiation site at bonding defect (left); with surface crack initiation (middle) and "as-built" specimen with multiple surface crack initiation sites (right).

"As-built" specimens exclusively fail from surface defects due to the high surface roughness inherent to the additive manufacturing process. Based on the SEM images the initial crack length respectively fracture plane for "as-built" specimens cannot be determined explicitly. It is expected, that the initial crack length corresponds to the maximum profile height R_t of additive manufactured surfaces. In the case of additive manufactured Ti-6Al-4V, the maximum profile height is $R_t = 90\ \mu m$.

Polished specimens show failure from internal bonding defects as well as surface failures. Failures caused by bonding defects in the region near the endurance limit (σ_{max} = 400 – 600 MPa) can be clustered into two groups. Early failure occurs at $N < 10^6$ cycles for near-surface defects and late failure at $N > 10^6$ cycles for remote-surface defects. The distinct differences in defect size and location cause the high scatter of the HCF data near the endurance limit.

For further investigation of the fatigue behavior using the Kitagawa-Takahashi diagram in section 3.4 the bonding and surface defects from the polished specimens were magnified and their projected crack initiation sites respectively fracture planes analyzed. The resulting defect area was determined using the estimation approach of MURAKAMI for irregular shaped cracks [Mur02].

3.3. Fatigue crack propagation threshold

The whole crack growth curve over all crack growth regimes was determined by measuring crack propagation rates as described in section 2.3. The threshold value of the stress range intensity factor ΔK_{th} at a crack growth rate of $da/dN = 10^{-7}$ mm/cycle was calculated by interpolation of the experimental data for values of $da/dN \leq 4 * 10^{-7}$ mm/cycle (Fig. 4). The calculated threshold value of $\Delta K_{th} = 3.48$ MPa $m^{1/2}$ is in good agreement with earlier crack propagation rate investigations of laser additive manufactured Ti-6Al-4V by LEUDERS [Leu12].

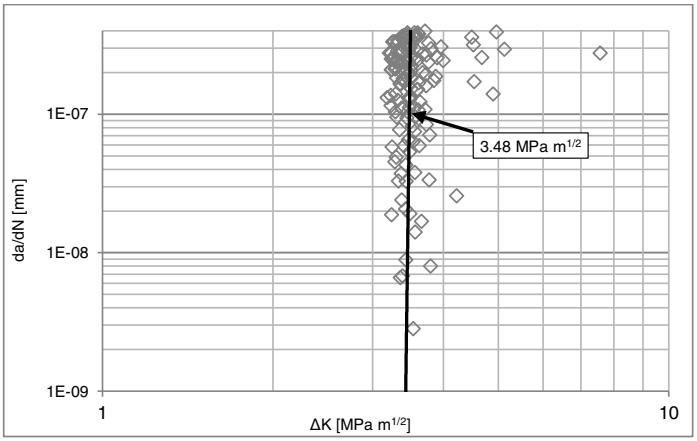

Fig. 4. Determination of stress intensity factor threshold ΔK_{th}.

3.4. Fatigue limit described by Kitagawa-Takahashi diagram and El Haddad and Topper approach

The influence of the crack length a of microscopic as well as macroscopic cracks on the maximum applicable stress range before failure can be described by the Kitagawa-Takahashi diagram (Fig. 5) [Kit76]. The diagram describes the stress range for crack propagation in the area of long cracks and low stresses as a function of a through:

$$\Delta\sigma(a) = \frac{\Delta K_{th}}{Y\sqrt{\pi a}} \tag{1}$$

and for short cracks through:

$$\Delta\sigma = \Delta\sigma_{fat} \tag{2}$$

where $\Delta K_{th}$is the threshold value, Y the geometrical correction factor and $\Delta\sigma_{fat}$ the fatigue limit of the material without cracks. Using the modified approach by EL HADDAD and TOPPER [Had79] the stress range is formulated more conservatively by:

$$\Delta\sigma(a) = \frac{\Delta K_{th}}{Y\sqrt{\pi(a + a_0)}} \tag{3}$$

respectively

$$\Delta\sigma(a) = \Delta\sigma_{fat}\sqrt{\frac{a_0}{a_0 + a}} \tag{4}$$

which is applicable for short and long cracks by introducing a material constant a_0:

$$a_0 = \frac{1}{\pi}\left(\frac{\Delta K_{th}}{Y\Delta\sigma_{fat}}\right)^2 . \tag{5}$$

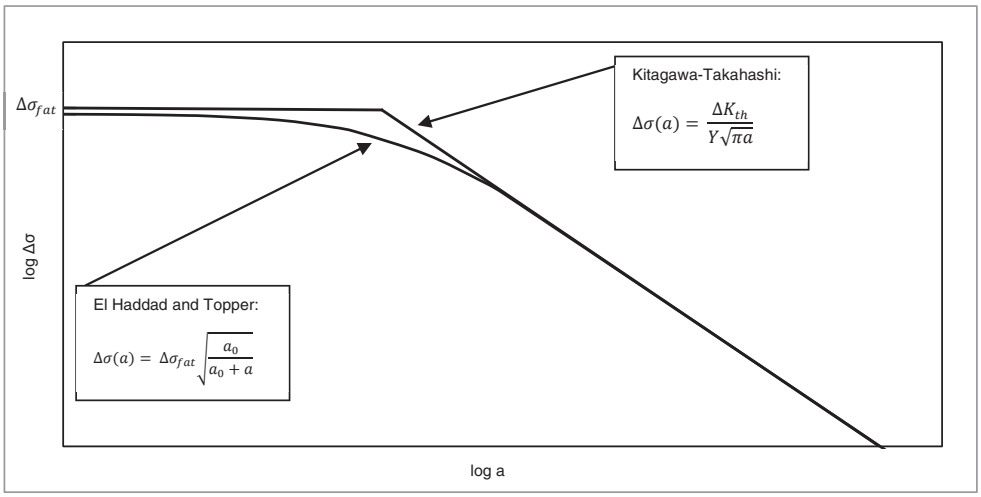

Fig. 5. Kitagawa-Takahashi diagram with El Haddad and Topper approach.

Due to the varying experimental set ups between HCF and Crack propagation tests as well as different defect geometries causing specimen failure multiple geometrical correction factors have to be considered. For the correction factor of bonding defects the "penny shaped" approach of MURAKAMI is used (equation 6) [Mur02]. The correction factor for surface defects in HCF specimen is calculated by the approach of GROSS and SEELIG (equation 7) [Gro11] and for CT-specimens according to ASTM E 399 (equation 8) [AST09]:

$$Y = \frac{2}{\pi}, \tag{6}$$

$$Y = 1.211 - 0.186\sqrt{\sin(\theta)}\,, \tag{7}$$

$$Y = \frac{\left(2 + \frac{a}{W}\right)\left[0.866 + 4.64\frac{a}{W} - 13.32\left(\frac{a}{W}\right)^2 + 14.72\left(\frac{a}{W}\right)^3 - 5.6\left(\frac{a}{W}\right)^4\right]}{\left(1 - \frac{a}{W}\right)^{3/2}} \tag{8}$$

with θ being the angle of the crack front to the specimen surface and W being the width of the CT-specimen. The calculation of the representative crack length for bonding defects is calculated by the "penny shaped" approach after MURAKAMI [Mur02]:

$$a = \sqrt{\frac{area}{\pi}} \tag{9}$$

with $area$ being the projected fracture plain determined as described in section 3.2.

To plot experimental data with unequal Y values, as applicable for the determined tests data, in one single Kitagawa-Takahashi diagram an equivalent crack length a_{equ} (equation 10) is introduced. a_{equ} allows to consider different geometrical correction factors for volume and surface defects (compare [Koe12]) with a_{equ} being:

$$a_{equ} = aY^2. \tag{10}$$

Using the equivalent crack length in the description of the stress range leads to the following transformation of the El Haddad and Topper approach:

$$\Delta\sigma(a_{equ}) = \Delta\sigma_{fat}\sqrt{\frac{a_{0equ}}{a_{0equ} + a_{equ}}} \tag{11}$$

with

$$a_{0equ} = \frac{1}{\pi}\left(\frac{\Delta K_{th}}{\Delta\sigma_{fat}}\right)^2. \tag{12}$$

In Fig. 6 the experimental data from the HCF and the crack propagation tests are shown in a Kitagawa-Takahashi diagram. In the diagram the Kitagawa-Takahashi curve (dashed line) as well as the El Haddad and Toper approach (solid line) are plotted over the equivalent crack length a_{equ}. Specimen failures from bonding as well as surface defects for polished HCF specimens are plotted in hollow circles. Additionally data from the crack propagation tests is added to the Kitagawa-Takahashi diagram. Defining the crack growth rate of $da/dN = 10^{-7}$ mm/cycle as the threshold below which crack growth effectively terminates, the data is divided in specimen failure (hollow grey diamonds) for a crack growth rate of $da/dN \geq 10^{-7}$ mm/cycle and specimen "run out" (filled black diamonds) for a rate of $da/dN < 10^{-7}$.

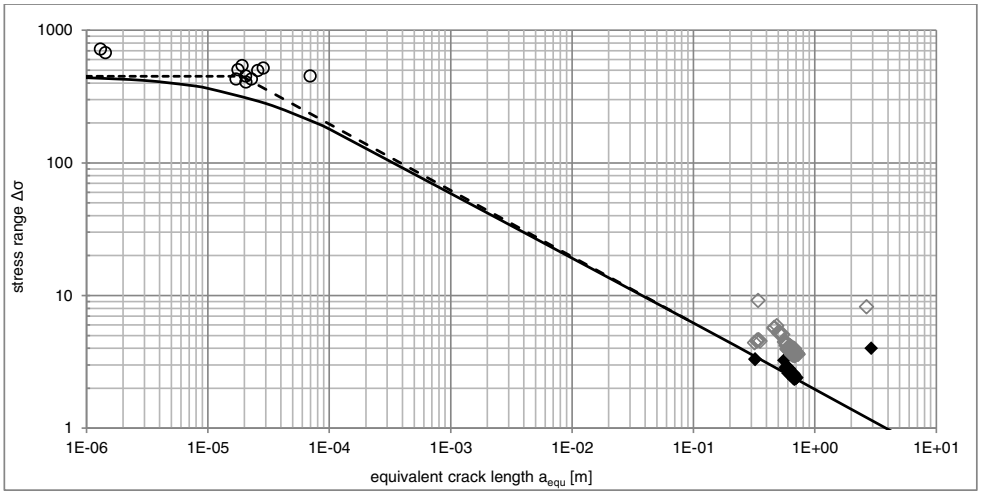

Fig. 6. Kitagawa-Takahashi diagram based on the experimental data from HCF and crack propagation tests.

4. Simulation

Additional to experimental investigations of fatigue properties, a simulation of the fatigue limit of laser additive manufactured Ti-6Al-4V was performed. The simulation was conducted in the LEFM-software AFGROW. For the model set up the experimental details of the HCF tests were duplicated simulating cylindrical specimen under a load ratio of R = 0.1. The material model was based on earlier experimental investigations of static and dynamic material properties [Wyc12, Wyc13], literature review [Bra10, Gre13, Leu12, Vlc07] and the determined crack propagation curve (section 2.3). An overview of selected material properties of laser additive manufactured Ti-6Al-4V used for the simulation is shown in Table 1.

Table 1. Selected material parameters used in fatigue limit simulation of laser additive manufactured Ti-6Al-4V.

Parameter		Value	
Ultimate strength	σ_U	1140	MPa
Yield strength	σ_Y	1070	MPa
Young's Modulus	E	110	GPa
Plain strain fracture toughness	K_{IC}	73	MPa $m^{1/2}$
Crack propagation threshold	ΔK_{th}	3.48	MPa $m^{1/2}$

Fig. 7 shows the result of the fatigue limit simulation additional to experimental data and the El Haddad and Topper curve in the Kitagawa-Takahashi diagram. The hollow items (square and triangle) represent the simulated minimum stress range at which failure occurs depending on crack lengths a_{equ}. Squares indicate failure from surface cracks, triangles representing failure from volume defects such as bonding defects in additive manufactured Ti-6Al-4V. The dotted line shows the interpolated values of the simulation results in the Kitagawa-Takahashi diagram.

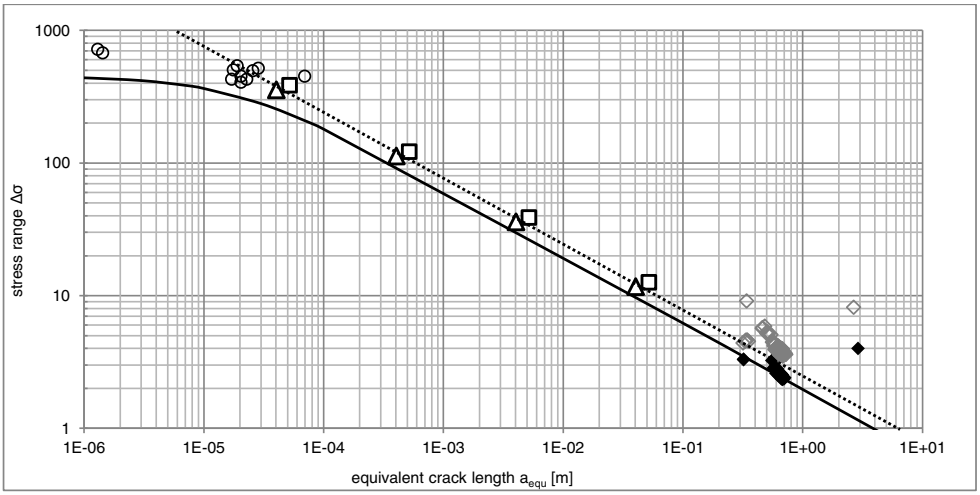

Fig. 7. Kitagawa-Takahashi with experimental data and results from the LEFM simulation.

5. Conclusions

The HCF tests show good fatigue properties of laser additive manufactured Ti-6Al-4V with an endurance limit of 500 MPa. Although the endurance limit diminishes for material in "as-built" condition, due to the process inherent high surface roughness, fatigue properties seem suitable for many applications in the aviation and medical industry. The tests show, that with consistent defect type the fatigue properties of additive manufactured titanium experiences low scatter (Fig. 2). High scatter in the region near the endurance limit, however, is caused by variants of defect type, sizes and location (Fig. 2).

To assess the influence of different defect parameters on the fatigue endurance, further fracture mechanical investigations were carried out. Using compact-tension specimens, the crack propagation curve over all the crack regimes as well as the propagation threshold was determined. With 3.48 MPa $m^{1/2}$ the determined stress intensity threshold ΔK_{th} is in good agreement with values of earlier investigations on laser additive manufactured Ti-6Al-4V [Leu12]. To evaluate the experimental results concerning the endurance limit depending on initial crack sizes, the data was plotted in a Kitagawa-Takahashi diagram. Comparing the experimental results with the Kitagawa-Takahashi and the El Haddad and Topper approaches it shows that these theories estimate the endurance limit for long cracks, as present in CT-specimens, too conservatively. It seems that the fatigue life in the case of laser additive manufactured specimen is dominated by the crack initiation stage which is attributable to the microstructure. The very fine microstructure of laser additive manufactured Ti-6Al-4V seems to influence the fatigue life positively compared to the models of Kitgawa-Takahashi and El Haddad and Topper. Details on the typical microstructure of laser additive manufactured parts can be found in [Bra10, Wir05, Wyc13]. Failures from smaller initial cracks presented by surface and bonding defects in HCF specimens, however, are represented by the Kitagawa-Takahashi approach quite accurately. Though former studies have shown that the endurance limit of small cracks is estimated more precisely by the El Haddad and Topper approach [Had79, Yat87], the discrepancy in this work might also be explained by the domination of the failure by the crack initiation stage as well as by the small sample size of investigated specimen.

Besides experimental investigations, a simulation with LEFM-software was performed. The simulation model was based on the HCF test including simulation of surface and volume defects with equal crack lengths. The small variation in simulation

results between surface and volume cracks are attributed to the different underlying model-theories in the software. The interpolated simulated endurance limit is in strong agreement with the experimental data for large cracks. The simulated endurance limit for small cracks, however, is overestimated. Due to the linear approach of the simulation, the overestimation of the endurance limit for short cracks was expected. Non-linear effects as well as micro-crack propagation below the stress intensity threshold ΔK_{th} are mostly not considered.

Based on the experimental data, the derived Kitagawa-Takahashi and El Haddad and Topper approaches as well as the analytical LEFM simulation, the fatigue limit of defect afflicted laser additive manufactured Ti-6Al-4V can be predicted very reliably. LEFM simulation software predicts the fatigue life for parts with large initial defects very precisely, overestimates, however, the fatigue life for smaller cracks. For smaller initial defects, the El Haddad and Topper approach gives a good conservative assessment of the fatigue limit.

Acknowledgements

Part of this work was supported by the German Federal Ministry of Education and Research (BMBF) within the frame of the project 03CL20B. The authors would like to thank the BMBF as well as the PTJ project management agency for their support. The responsibility for the content of this publication lies with the authors.

References

[AST00] Standard Test Method for Measurement of Fatigue Crack Growth Rates, ASTM – E 647, ASTM, 2000.

[AST07] Standard Practice for Conducting Force Controlled Constant Amplitude Axial Fatigue Tests for Metallic Materials, ASTM – E 466, ASTM, 2007.

[AST09] Standard Test Method for Linear-Elastic Plane-Strain Fracture Toughness Kic of Metallic Materials, ASTM – E 399, ASTM, 2009.

[Bra10] Brandl, E., "Microstructural and mechanical properties of additive manufactured titanium (Ti-6Al-4V) using wire", Shaker Verlag, Aachen, 2010.

[DIN78] DIN 50 100, Dauerschwingversuch: Begriffe, Zeichen, Durchführung, Auswertung, DIN, 1978.

[Emm11a] Emmelmann, C.; Scheinemann, P.; Munsch, M.; Seyda, V., "Laser Additive Manufacturing of modified implant surfaces with osseointegrative characteristics", Physics Procedia, Volume 12, Part A, 2011, Pages 375-384.

[Emm11b] Emmelmann, C., Sander, P., Kranz, J., Wycisk, E.,"Laser Additive Manufacturing and Bionics: Redefining Lightweight Design", Physics Procedia 12, Part A, 2011.

[Gre13] Greitemeier, D., Schmidtke, K., Holzinger, V., Dalle Donne, C., „Additive Layer Manufacturing og Ti-6AL-4V and ScalmalloyRP: Fatigue and Fracture", Proceedings of 27th ICAF Symposium, Jerusalem, 5-7 June 2013.

[Gro11] Gross, T., Seelig, T., "Bruchmechanik: Mit einer Einführung in die Mikromechanik", Heidelberg, Springer, 2011.

[Had79] El Haddad, M. H., Topper, T. H., Smith, K. N., "Prediction of non propagating cracks", Engineering Fracture Mechanics, Vol. 11, 1979, Pages 573-584.

[Hoo12] Van Hoorweder, B., et. al., „Analysis of Fracture Thoughness and Crack propagation of Ti6Al4V Produced by Selective Laser Melting", Advanced Engineering Materials, 2012, 14 No.1-2, Pages 92-97.

[Kit76] Kitagawa, H., Takahashi, S., "Applicability of fracture mechanics to very small cracks or the cracks in the early stages". Proceedings of 2nd internatonal conference on mechanical behavior of materials, Boston, Pages 627-631.

[Koe12] Koehler, B., Bomas, H., Leis, W., Kallien, L., „Endurance limit of die-cast magnesium alloys AM50hp and AZ91hp depending on type and size of internal cavities", International Journal of Fatigue 44, 2012, Pages 51-60.

[Leu12] Leuders, S., et. al., „On the mechanical behaviour of titanium alloy TiAl6V4 manufactured by selective laser melting: Fatigue resistance and crack growth performance.", International Journal of Fatigue 48, 2013, Pages 300-307.

[Mur02] Murakami, Y., "Metal fatigue: Effects of Small Defects and Nonmetallic Inclusions, Oxford, Elsevir, 2002.

[Vlc07] Vlcek, J., "Property Investigation of Ti-6Al-4V Produced by Additive Manufacturing", TMS 2007, 136th annual meeting & exhibition, Minerals, Metals and Materials Society / Light Metals, 2007, Pages 89-98.

[Wir05] Wirtz, T., „Herstellung von Knochenimplantaten aus Titanwerkstoffen durch Laserformen", Aachen, 2005.

[Woh13] Wohlers, T., "Wohlers Report 2013", Wohlers Associates, Inc., Fort Collins, Colorado, USA, 2013.

[Wyc12] Wycisk, E., Kranz, J., Emmelmann, C., " Fatigue Strength of Light Weight Structures produced by Laser Additive Manufacturing in TiAl6V4", Proceedings of 1st International Conference of the International Journal of Structural Integrity, Porto, 15.-28.06.2012.

[Wyc13] Wycisk, E., Emmelmann, C., Siddique (V), S., Walther. F., "High Cycle Fatigue (HCF) Performance of Ti-6Al-4V Alloy Processed by Selective Laser Melting", Advanced Materials Research Vols. 816-817, 2013, Pages 134-139.

[Yat87] Yates, J. R., Brown, M. W., "Prediction of the length of non-propagating fatigue cracks", Fatigue of Engineering Materials, Fatigue Fract. Engng Mater. Struct. Vol. 10, No. 3, 1987, Pages 187-201.